

DIFFERENCES IN EMULSION POLYMERIZATION FOULING BETWEEN ACRYLATES AND VINYL ACETATE STUDIED IN-SITU WITH A QUARTZ CRYSTAL MICROBALANCE (QCM)

*K. M. Hoffmann¹, A. Langhoff¹, J. Adams¹, H. A. Huellemeier²,
W. Augustin², S. Scholl² and D. Johannsmann¹

¹ Institute of Physical Chemistry, Clausthal University of Technology, Arnold-Sommerfeld-Str. 4,
38678 Clausthal-Zellerfeld, Germany, kevin.marvin.hoffmann@tu-clausthal.de

² Institute of Chemical and Thermal Process Engineering, Technische Universität Braunschweig,
Langer Kamp 7, 38106 Braunschweig, Germany

ABSTRACT

Fouling is a severe problem in emulsion polymerization, which – among other consequences – currently prevents polymerization in continuous flow reactors. Measuring the early stages of fouling (<10 µm) can be challenging due to the low sensitivity of traditional fouling detection methods (i.e., thermal resistance and pressure drop). In comparison, measurements conducted with a highly sensitive quartz crystal microbalance enable the *in-situ* monitoring of fouling and the detection of the initial layers fouling. In this study, a QCM-D (quartz crystal microbalance with dissipation monitoring) was configured to function as a heat transfer surface to compare the fouling of acrylates and vinyl acetate. For the acrylates, fouling is self-limiting such that the layer thickness is finite and within the range of the diameter of acrylate particles. Thus, for acrylates fouling can be described as the adsorption of a single layer of particles. For vinyl acetate, the fouling layers grow continuously and result in a thick coagulum. The mechanistic details associated with the difference between acrylates and vinyl acetate is the subject of ongoing investigations. Furthermore, this work also explores how QCM-D technology can contribute to the study of fouling in general.

INTRODUCTION

Fouling in Emulsion Polymerization

Emulsion polymerization accounts for the annual production of several million tons of polymer dispersions. After drying, these latices form paints, varnishes, coatings, or adhesives.^[1] Emulsion polymerization is a variant of a free-radical polymerization and occurs mostly inside micelles. The main components of an emulsion polymerization recipe are an emulsifier, monomer (possibly a mixture of monomers), water as the continuous phase, and a water-soluble initiator. The emulsifier self-assembles into micelles when the concentration is above the critical micelle concentration (CMC). Also, the emulsifier stabilizes the monomer droplets, where the latter have a size of a few micrometers. The monomer has a finite solubility in the aqueous phase, so that the water-

soluble initiator can start the reaction by attacking the monomer. The resulting oligomers diffuse into the micelles and continue to grow. This phase is termed “particle formation”. In the second phase, “particle growth”, monomer continues to diffuse from the droplets into the micelles, where it is incorporated into the growing latex particles. The reaction eventually slows down in the last phase, known as “monomer depletion”.^[2]

The process outlined above describes the polymerization of acrylates slightly better than the polymerization of vinyl acetate. In the latter case, the “protective colloid” composed of polyvinyl alcohol is grafted onto the vinyl acetate as polymerization proceeds and then stabilizes the particles against aggregation.^[3] Polyvinyl alcohol does not form micelles before the start of the polymerization.

Industry mostly employs what is called a semi-batch process.^[4] Monomer and other parts of the recipe are dosed into the reaction chamber as the reaction proceeds. Dosing allows more control over the process. In the batch process, all ingredients except the initiator are added to the reaction chamber at the start. Emulsion polymerization in a continuous flow reactor is challenging because reactor walls are quickly fouled. Designs for emulsion polymerization reactors which enable continuous-mode operation have been developed, but without wide-spread application.^[5]

Fouling often occurs on heat transfer surfaces, such as the walls of reaction vessels and heat exchangers, where a temperature differential between the surface and the bulk fluid is imposed.^[6] For emulsion polymerization, two types of fouling are to be distinguished, reaction fouling and particle fouling. Reaction fouling occurs when a radical (initiator, monomer, or oligomer) adsorbs to the surface. The reaction continues at the surface and the produced chains are attached to the surface.^[7] In particle fouling, latex particles formed in the bulk fluid adsorb to the surface rather than individual reaction precursors. The particles may adsorb individually or form coagulates, which then adsorb cooperatively.^[8]

There are several stages of fouling, namely initiation, transport, attachment, removal, and aging.^[9] The most important stages for emulsion polymerization fouling are transport, attachment, and removal. Following KERN and SEATON^[10], the rate of fouling ($\frac{dm}{dt}$) per unit area ($\text{kg}\cdot\text{m}^{-2}\cdot\text{s}^{-1}$) assuming a constant density (ρ_d , $\text{kg}\cdot\text{m}^{-3}$) and thermal conductivity (λ_d , $\text{W}\cdot\text{m}^{-1}\text{K}^{-1}$) is equal to:

$$\frac{dm}{dt} = \dot{m}_d - \dot{m}_r = \frac{dR_f}{dt} \rho_d \lambda_d \quad (1)$$

where \dot{m}_d is the rate of deposition ($\text{kg}\cdot\text{m}^{-2}\cdot\text{s}^{-1}$), \dot{m}_r is the removal rate ($\text{kg}\cdot\text{m}^{-2}\cdot\text{s}^{-1}$), and R_f is the thermal fouling resistance ($\text{m}^2\cdot\text{K}\cdot\text{W}^{-1}$). The KERN-SEATON model assumes that fouling is detected by a change in the thermal resistance of the fouling layer. Current measurement techniques, whether *in-situ* or *ex-situ*, cannot distinguish between particle fouling and reaction fouling. Fouling deposits on the reactor walls can be analyzed in detail after the reaction but this *a posteriori* analysis does not usually clarify the mechanisms leading to deposition.

The monitoring of fouling (usually integral not local), based on the use of temperature or pressure sensors, suffers from limited sensitivity.^[11] Thus, thin deposit layers formed during the early phases of fouling cannot be studied. It is important to comprehend the early phases of fouling in order to understand the subsequent fouling stages. Therefore, more sensitive sensors are needed, such as the quartz crystal microbalance (QCM). The sensitivity of the QCM enables the detection of a monolayer of particles. Also, data beyond the mass coverage at the sensor surface ($\mu\text{g}\cdot\text{cm}^{-2}$) is available with measurements of energy dissipation (QCM-D). Dissipation is among the non-gravimetric parameters. Further non-gravimetric parameters, e.g. roughness, softness or compliance of the sample, are inferred from the comparison of the shifts in frequency and bandwidth from multiple overtones. These non-gravimetric parameters certainly require interpretation, but this is possible in many cases.^[12]

The QCM monitors fouling in-situ

The QCM is an acoustic sensor which infers changes in mass from shifts in the resonance frequency of a piezoelectric plate. The plate oscillates at frequencies in the MHz range. Because the vibration occurs in the thickness-shear mode, the resonator surface emits transverse waves only, which decay in the liquid. The finite decay length (a few hundred nanometers) turns the QCM into surface-sensitive instrument. Conversely, the QCM cannot quantify a layer thickness, if the latter exceeds the decay length.

SAUERBREY first proposed to use quartz resonators for sensing in 1959.^[13] He formulated the

SAUERBREY equation, which relates the deposited mass per unit area to the shift in frequency as

$$-\frac{\Delta f}{f_{\text{ref}}} = -\frac{\Delta f}{n f_0} = \frac{\Delta m}{m_q} = \frac{\rho_f}{m_q} d_f \quad (2)$$

where Δf is the shift in frequency relative to the reference state with frequency f_{ref} (Hz), Δm ($\text{kg}\cdot\text{m}^{-2}$) is the change in mass per unit area (often in units of $\mu\text{g}\cdot\text{cm}^{-2}$), m_q ($\text{kg}\cdot\text{m}^{-2}$) is the mass per unit area of the resonator plate, n is the overtone order, and f_0 is the frequency of the fundamental overtone (Hz). m_q is given as $\frac{Z_q}{2 f_0}$ with $Z_q = 8.8\cdot 10^6 \text{ kg}\cdot\text{m}^{-2}\cdot\text{s}^{-1}$ the shear-wave impedance of the resonator plate. The change in mass (Δm) can be converted to the thickness of the deposited film, d_f (m), if the density of the film, ρ_f ($\text{kg}\cdot\text{cm}^{-3}$), is known. For polymers, the density of the film is known to be about $1 \text{ g}/\text{cm}^3$. The uncertainty in the density does not usually exceed the experimental uncertainty and thus, Δf is readily converted to d_f .

With the QCM-D it is possible to also track the shifts in half bandwidth, $\Delta\Gamma$ (Hz), which provide information about the deposits viscoelastic parameters (mostly its softness, possibly with some influence of the geometry). If $\Delta\Gamma$ is close to zero and if $\Delta f/n$ is the same on all overtones, a rigid film can be assumed, and the SAUERBREY approximation is valid. Conversely, if $\Delta\Gamma$ is similar in magnitude to $-\Delta f$, a viscoelastic film is present and the SAUERBREY equation does not hold.^[14] In those cases, frequency shift cannot be directly converted to layer thickness with the SAUERBREY equation.

Previous Work on Acrylates

Previous work has addressed the fouling of acrylates.^[12] The QCM was integrated into the wall of a small reactor (with a volume of 14 ml). The resonator plate was heated from the back with a ring-shaped thermal pad. The pad must be ring-shaped in order to not touch the resonator at the center. It would otherwise overdamp the vibration. Figure 1 shows a sketch.

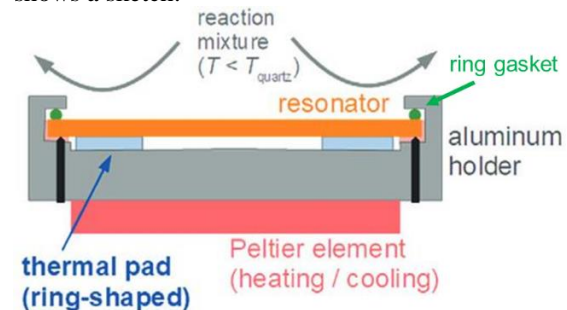


Figure 1: Sketch of the QCM configured as a heat transfer surface. Differing from this sketch, the resonator is mounted vertically, so that neither sediments nor bubbles accumulate on the resonator.^[12]

Challenges with this configuration include fluctuations in temperature and pressure, which deteriorate the signal. The noise level, typically a few Hz, is about 100 times greater than the noise level in more controlled environments. But the magnitude of the frequency shifts associated with fouling during emulsion polymerization (> 1 kHz) easily allows the toleration of this level of noise.

In previous experiments on acrylates, two different fouling scenarios have been observed.^[12] One fouling pathway produced a thin layer (less than $1\ \mu\text{m}$ in thickness), which protects the surface against further fouling. The other fouling pathway produced thick deposits shortly after the initiation of the polymerization reaction. Occasionally, there was a small peak in the resonance bandwidth prior to the main transition. Presumably, such a peak can be attributed to soft lumps of coagulum making contact with the resonator surface.

Objectives

The main target of this research is to try to characterize and understand the initial steps of the fouling process for different emulsion polymerization systems. With the QCM-D, one can follow the fouling process in situ and distinguish between thick or thin and rigid or soft layers. Beside the system of acrylates, vinyl acetate will be investigated. It is more water soluble, leans more to branching and has a lower T_G compared to the investigated system of butyl acrylate and methyl methacrylate. Further, this work should illustrate the strengths of the QCM-D in the research area of particulate and reaction fouling.

EXPERIMENTAL SECTION

Reaction Chamber

The reactor shown in Figure 2 had a volume of 21 ml. All reactions were carried out in batch mode. A semi-batch process requires a larger reactor volume. When including all reaction components in the recipe directly at the start, latex particles are formed more quickly than in semi-batch reactions. Thus, the reaction time, the temperature, and the viscosity are more difficult to control.

The QCM is integrated into the reactor wall which is connected to a heating block. The heating block contains the resonator.

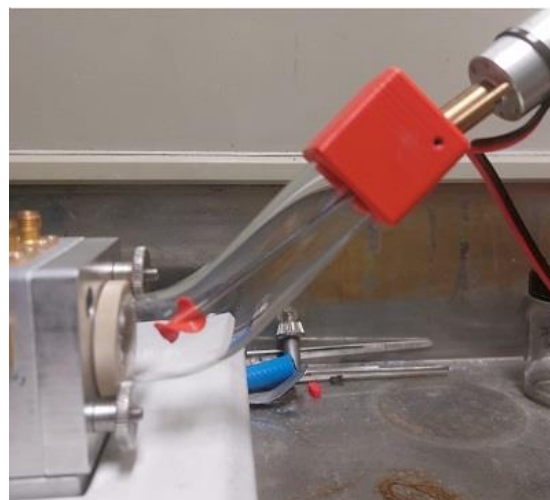


Figure 2: Reactor with stirrer integrated into the lid. The lid contains small holes for adding the initiator.

To start the reaction, the temperature of the heating block is increased to $85\ ^\circ\text{C}$. The temperature here is a nominal temperature as reported by a thermocouple integrated into the base of the heating block. The block transfers the heat to the resonator across a ring-shaped thermal pad. The resonator is the only heat-transfer surface in the system. The rest of the reactor was not jacketed. With this configuration, the temperature of the resonator (circa $85\ ^\circ\text{C}$) is always greater than the temperature of the reaction mixture (around $66\ ^\circ\text{C}$) such that fouling *only* occurs at the resonator surface, which is important for the data interpretation.

This experimental setup results in a few differences from industrial emulsion polymerization processes. First, an overhead agitator is used to ensure the reaction volume is well stirred, but the hydrodynamics are not controlled to the extent which would be desired in industry. Secondly, reactors in industrial settings often remove the heat produced by the exothermic reaction, so the reactor walls are at a lower temperature than the reaction mixture. They cool the reaction mixture rather than heating it, and they do so in a poorly controlled way. Yet this work targets the study of fouling mechanisms, rather than mimicking industrial polymerization conditions.

Materials and Methods

Reactions were conducted with ultrapure water, obtained from an Arius 611 VF apparatus (Sartorius). The reactants and the reactor were flushed with nitrogen for at least five minutes before the start of the reaction to remove oxygen. All monomers other than acrylic acid were purged of the inhibitor, which was 4-methoxyphenol (MEHQ) with an inhibitor removal resin (Aldrich). Stabilization was accomplished with nonionic emulsifiers. A short-chain emulsifier (Lutensol AT50, BASF) was chosen for the acrylates. A

protective colloid (polyvinyl alcohol) was chosen for vinyl acetate. Quartz sensors with gold electrodes and a fundamental frequency of 5 MHz with a diameter of 1 inch were used (obtained from Quartz Pro). Resonance curves were acquired with a vector network analyzer (N2PK, Makarov Instruments). The data acquisition software fits phase-shifted Lorentzians to the admittance traces, thereby determining the resonance frequency and the resonance bandwidth.

The reaction time varied between 90 and 120 min. A high solids content (> 50 %) was not the target of investigations as is common in industry.

For the polymerization of the acrylates, water, sodium bicarbonate (NaHCO₃, Acros), butyl acrylate (BA, Aldrich), methyl methacrylate (MMA, Acros), and acrylic acid (AA, Fluka) were fed into the reactor. The monomer ratio was 0.495:0.495:0.01 (BA:MMA:AA) by weight. The glass transition temperature of this copolymer, as calculated with the FOX equation^[15], was $T_G \approx 10$ °C. After stirring the mixture for 5 minutes, the emulsifier was added. After heating for 10 minutes, sodium persulfate (NaPS, Merck) was added to initiate the reaction. A typical recipe is shown in Table 1.

Table 1: A typical recipe for the polymerization of acrylates (a target solids content of 35 % w/w selected as an example).

Material	Content [pphm]*
MMA (monomer 1)	49.5
BA (monomer 2)	49.5
AA (monomer 3)	1.0
Lutensol AT50 (emulsifier)	7.5
H ₂ O (aqueous phase)	194.4
NaHCO ₃ (buffer)	0.4
NaPS (initiator)	5.0

*pphm: parts per hundred monomer

For the polymerization of vinyl acetate, the reactor was filled with water, NaHCO₃ and vinyl acetate (VAc, Merck). The emulsifier polyvinyl alcohol (PVOH, $M_w = 115000$ g·mol⁻¹, degree of hydrolysis 88 %, VWR Chemicals), was added. This mixture was stirred and heated for 10 minutes before the initiator NaPS was added. The recipe is shown in Table 2.

The glass temperature of the resulting polymer was $T_G \approx 47$ °C as determined with differential scanning calorimetry. This T_G is higher than the T_G of the acrylates. $T_G \approx 47$ °C is still much below the reaction temperature, which was between 70 °C and 80 °C.

Table 2: A typical recipe for the polymerization of vinyl acetate (a target solids content of 35 % w/w selected as an example).

Material	Content [pphm]*
VAc (monomer)	100
PVOH (protective colloid)	11.2
H ₂ O (aqueous phase)	205.2
NaHCO ₃ (buffer)	0.4
NaPS (initiator)	4.5

*pphm: parts per hundred monomer

The main variable parameters in the recipe were the amount of water and the amount of monomer, respectively, which controls the solids content. The target solids content ranged from 10 % w/w to 35 % w/w in steps of 5 %.

RESULTS AND DISCUSSION

Polymerization of Acrylates

Figure 3 shows a data set from the polymerization of acrylates, where a thin fouling layer was formed after about 30 minutes of reaction time. The thin layer is characterized by a SAUERBREY behavior, as evidenced by $\Delta f/n$ being much smaller than $-\Delta f/n$ and, also, by $-\Delta f/n$ being similar on the different overtones. We call such layers “thin in the Sauerbrey sense”. A frequency shift of $-\Delta f/n \approx 2$ kHz corresponds to a layer thickness of $d_f \approx 400$ nm (based on (2), assuming a film density of 1 g/cm³) which is in the range of the particle diameters.

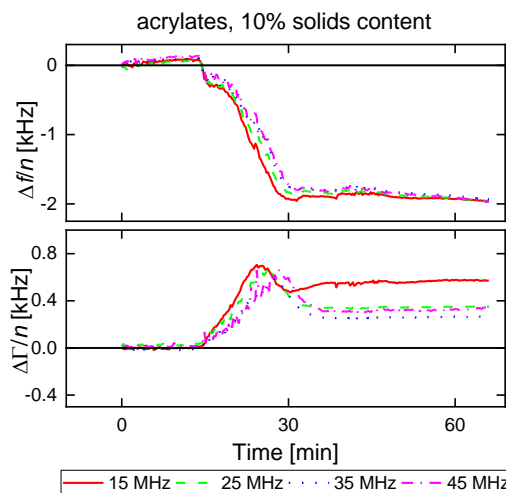


Figure 3: Overtone-normalized shifts in frequency, $\Delta f/n$, and half bandwidth, $\Delta \Gamma/n$, acquired during a polymerization of acrylates at a 10 % w/w solids content.

The transient maximum in $\Delta \Gamma$ might at first sight be interpreted as the signature of a so called “film resonance”. When films growing in thickness reach a thickness of $\lambda/4$ (λ the wavelength of shear sound), the film forms a resonator of its own (similar to a vibrating reed). The bandwidth then goes

through a maximum and the frequency transiently increases.^[16] The maximum seen in Figure 3 does not correspond to a coupled resonance of this type. There is no increase in frequency and the order, in which the different overtones traverse the maximum, is at variance with what is expected for a film resonance. Rather, the maximum is indicative of a compaction, setting in after about 28 min. The compaction is driven by wet sintering, that is, by the surface energy between the polymer and the water. This interpretation was corroborated with a numerical simulation.^[16]

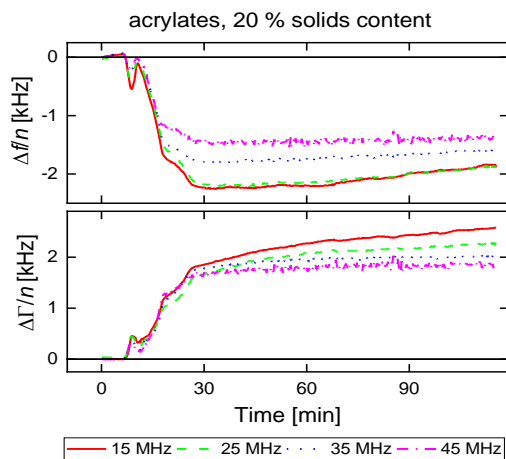


Figure 4: Overtone-normalized shifts in frequency, $\Delta f/n$, and half bandwidth, $\Delta\Gamma/n$, acquired during a polymerization of acrylates, 20 % w/w solids content.

Figure 4 shows an example, where the fouling layer does not form a *thin* film during acrylate polymerization. One finds $-\Delta f/n \approx \Delta\Gamma/n$ in the final state. Also, the overtone-normalized frequency shifts differ between overtones. It is difficult to quantitatively analyze these data in terms of a film thickness or a shear modulus, but it can be safely stated that this sample is not a rigid film.

A small peak is seen at the beginning (after around 10 minutes) for both the frequency and the bandwidth. Presumably, a small piece of coagulum was attached but was removed shortly after deposition. Removal of fouling material, as claimed in the KERN-SEATON model (Equation 1), is the exception for acrylates. Most of the time, fouling layers from acrylate polymerization continuously grow in thickness. Of course, the time evolution of $\Delta f/n$ might be the consequence of a dynamic situation with deposition and removal occurring simultaneously, at least in principle.

While this layer is not thin and not rigid, the resonances are still visible even after the layer thickness had increased to beyond what can be resolved by the QCM. This is in contrast to data associated to vinyl acetate (Figure 5), where the

bandwidth increases to the extent that resonance curves can no longer be fitted to the electrical admittance traces.

Polymerization of Vinyl Acetate

QCM monitoring of the fouling of vinyl acetate polymerization was less regular in the sense of a SAUERBREY behavior than monitoring of acrylates. The target solids contents were the same as in the case of the acrylates.

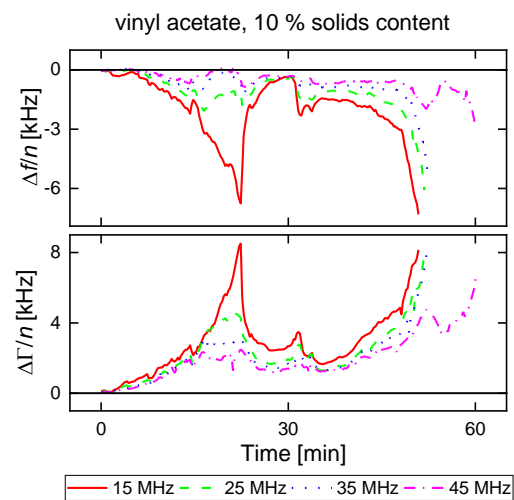


Figure 5: Overtone-normalized shifts in frequency, $\Delta f/n$, and half bandwidth, $\Delta\Gamma/n$, acquired during a polymerization of vinyl acetate, 10 % w/w solids content.

Figure 5 shows an example, where the target solids content was 10 % w/w. After 50 minutes of reaction, the magnitude of the resonance bandwidth became so high that the QCM was no longer operational. The data acquisition software can no longer fit resonance curves to the traces of the electrical admittance. No such behavior is seen for the acrylates. At $t \approx 20$ minutes after the initiation of the reaction, a transient peak in the first overtone is observed. Such large transient maxima were only seen for low solids contents. Transient features are also seen for the acrylates ($t \approx 10$ minutes in Figure 4), but these are much smaller in magnitude. Most likely, it is a thick deposit of coagulum attached and detached from the resonators surface as also seen for the acrylates.

Figure 6 shows an example where the concentration of vinyl acetate is higher (target solids content of 35% w/w). These data are noisier than the data for the acrylates. However, the fluctuations do not reflect instrumental noise, but rather originate from the sample. Presumably, small clusters of coagulum repeatedly attach and detach from the resonator surface.

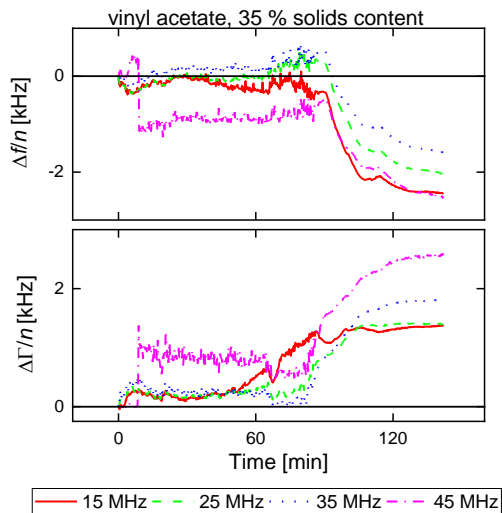


Figure 6: Overtone-normalized shifts in frequency, $\Delta f/n$, and half bandwidth, $\Delta\Gamma/n$, acquired during a polymerization of vinyl acetate, 35 % w/w solids content.

In Figure 6, the frequency shift turns positive at $t \approx 70$ min. $\Delta f/n > 0$ typically is attributed to “elastic coupling”.^[14] It is caused by stiff objects making contact with the resonator surface across narrow contact points. Writing the resonance frequency as $(\kappa_{\text{eff}}/m_{\text{eff}})^{1/2}$ with κ_{eff} an effective spring constant and m_{eff} an effective mass, a decrease in resonance frequency is naturally explained with inertial forces

exerted onto the resonator by the sample, which is the conventional case.^[14] But there are also cases where the sample makes contact with the resonator across narrow contact points, thereby increasing its effective stiffness (increasing κ_{eff}) and increasing the frequency. Positive frequency shifts are mostly observed with granular media (sand piles, spheres). Presumably, point contacts of this kind existed in the experiment shown in Figure 6.

Comparison

Figure 7 provides a comparison of experiments conducted with acrylates and vinyl acetates at the varying target solids contents (increases from top to bottom). The figure not only shows the influence of the solids content (which is small), but also illustrates the variability of the results between the two monomer systems. With Acrylates, we either see stable thin films in the Sauerbrey sense or films which are not rigid ($-\Delta f/n \approx \Delta\Gamma/n$). One of this two cases is always seen and is also reproducible. The stable thin films prevent the the layer against further fouling. For vinyl acetate, we see much more fluctuations between single solids contents. The QCM is very often losing the resonance frequencies and no data can be collected after some time. This data is less reproducible, but for early stages of the reaction, similar patterns can be seen which can be interpretate as reaction fouling processes.

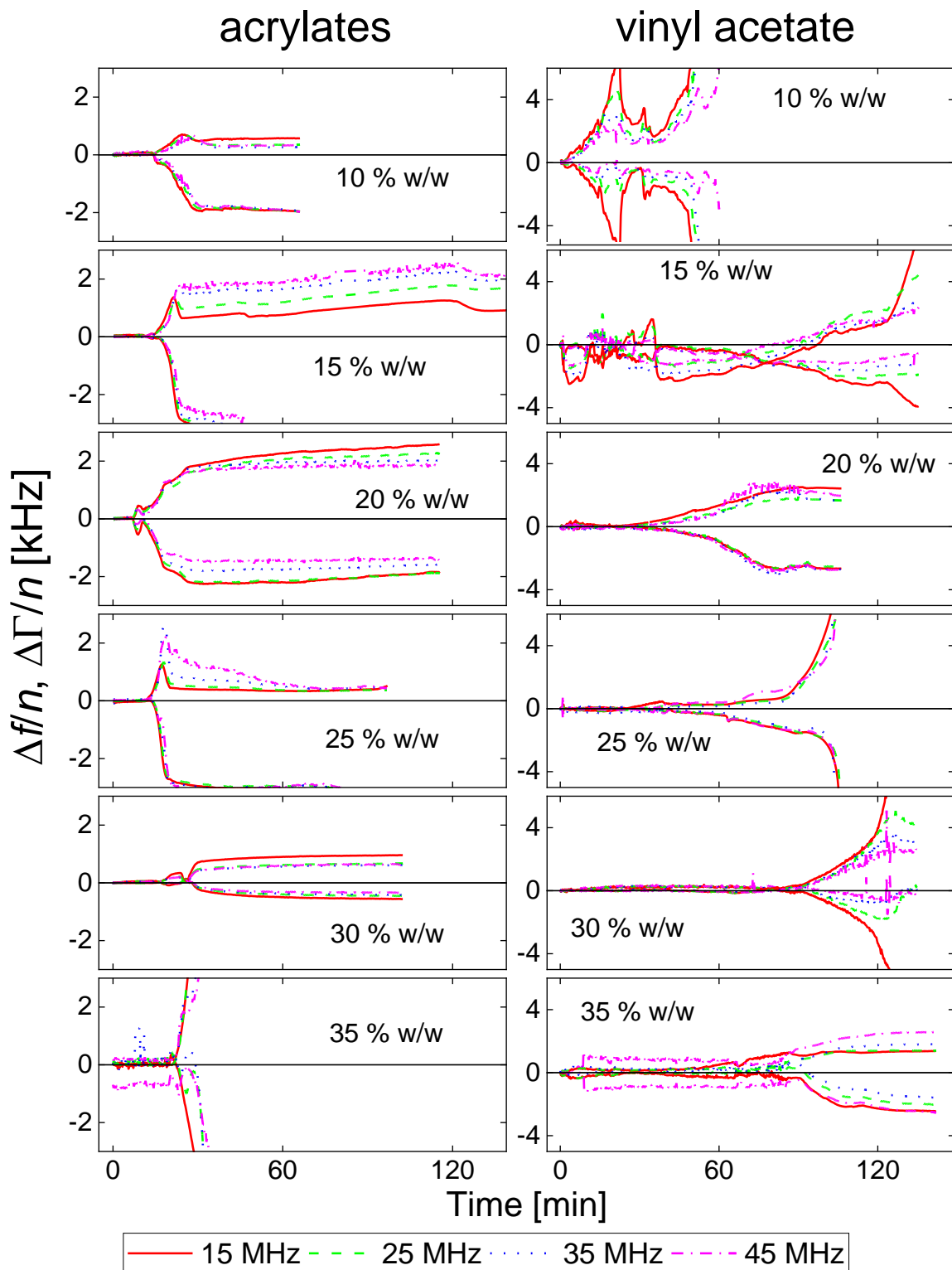


Figure 7: Overview of overtone-normalized shifts in frequency, $\Delta f/n$, and half bandwidth, $\Delta\Gamma/n$ of acrylates and vinyl acetate. Acrylates more often form thin films than vinyl acetate.

Figure 8 shows one data set (adapted from Ref. 11), where the BA content was only 10%. This material has a T_G comparable to the T_G of the vinyl acetate samples. This data set proves that the difference in fouling behavior between acrylates and

vinyl acetate do not primarily – or at least not only – related to differences in the T_G . These samples also produced films of finite thickness with compaction after the initial adsorption. The data was also more

reproducible than the data associated with vinyl acetate.

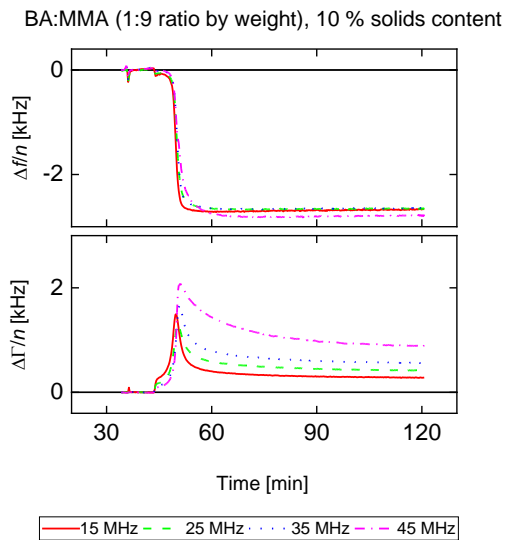


Figure 8: Overtone-normalized shifts in frequency, $\Delta f/n$, and half bandwidth, $\Delta \Gamma/n$, acquired during a polymerization of acrylates with a T_G similar to the T_G of the vinyl acetate. Differing from the recipe shown in Table 1, the BA/MMA ratio was 1:9. Also an anionic emulsifier (Dowfax 2A1, BASF) was used. The target solids content was 10 % w/w.^[12]

Discussion

I: Features of the QCM data traces with relevance to fouling

- Ia) The most important question answered by the QCM data is whether or not the layer is a thin film in the SAUERBREY sense.
- Ib) A transient maximum in bandwidth, which occurs on the lowest overtones first, is indicative of a compaction stage.
- Ic) The QCM evidences irregular transient events within the fouling process. These may be slow and with large amplitudes, presumably caused by single large flocs of coagulum, or fast and with smaller amplitudes, probably due to smaller clusters of particles.
- Id) Occasional occurrences of positive frequency shifts are indicative of point contacts with rather stiff objects (“elastic coupling”).
- Ie) Thick layers may or may not broaden the resonance to the extent that the fitting software does not longer recognize the resonance.

II: Differences between acrylates and vinyl acetate

- IIa) The acrylates more often show self-limiting fouling behavior with stable layers of finite thickness. Exceptions are present for both monomer systems.
- IIb) Acrylates behave more regularly. Vinyl acetate shows large and small transient maxima.
- IIc) Vinyl acetate occasionally leads to positive frequency shifts.

II d) The regular transient maxima with a well-defined sequence in overtone order (low \rightarrow high) are only seen with the acrylates.

II e) Only vinyl acetate lets the bandwidth increase to the extent, that the resonances can no longer be discerned.

In some cases, the two sets of findings can be related easily:

- The higher T_G allows for elastic coupling across narrow contacts between hard spheres and the resonator surface (positive Δf) (Id / IIc).
- Because vinyl acetate does not deform and coalesce in the same way as the acrylates due to the higher T_g , open clusters persist, which let the behavior be less regular (Ic).
- Because vinyl acetate is the stiffer material (that is, the material with the higher T_g), thick layers more easily overdamp the resonator in the final state than the layers formed by the acrylates (Ie).

The interpretation of the effect of the T_G only is questionable because the high- T_G acrylate did not behave like the vinyl acetate (see Figure 8). This material had been stabilized with an anionic emulsifier, though. Presumably, chemical pathways play a role equally important as T_G . This would indicate that reaction fouling is the dominant mechanism. The polymerization of vinyl acetate differs from the polymerization of acrylates in the following regards:

- Because the solubility of the monomer in water is higher, reaction fouling is more likely.
- Vinyl acetate contains more long-chain branches than acrylates.^[2,3] These slow down large-strain deformation during compaction more strongly than small-strain deformation.^[17,18] The effect of a high T_G is to be distinguished from the effect of long-chain branching in this regard. Long-chain branching can also lead to partial crosslinking and the formation of microgels.
- The protective colloid (polyvinyl alcohol) used in polymerization of vinyl acetate does not form micelles before polymerization starts. Therefore, in the early phases of particle formation, stabilization of the monomer is poor.

The effect of these differences between polymerization of vinyl acetate on fouling behavior will be clarified in further research.

CONCLUSIONS

Using a QCM-D integrated within a small reactor, it was shown that the polymerization of acrylates and vinyl acetate result in different fouling behaviors. Acrylates more often form stable thin films, as evidenced by a SAUERBREY-type response of the QCM. Acrylates undergo a compaction, which is not seen for vinyl acetate. Conversely, vinyl acetate often forms thick layers and its

behavior is more irregular than the behavior of the acrylates.

Among the factors of influence is the glass temperature. However, high- T_G acrylates did not behave like vinyl acetate. Presumably, reaction fouling plays a role. Reaction fouling is more likely for the vinyl acetate because of the better solubility in water, the long-chain branches, microgels, and the delayed formation of the stabilizing shell of polyvinyl alcohol.

For further research, a scale-up process is ongoing. A copolymer of vinyl acetate and vinylneodecanoate with a reaction volume of $V \approx 750$ ml will be used to investigate reaction and particulate fouling on a larger scale. This copolymer (~ 32 °C with a ratio of VAc 4:1 neovinyldecanoate) has a lower T_G than pure VAc (47 °C). With that, the main target is to start finding differences between acrylates and the co-polymer system which indicate to either reaction or particulate fouling.

ACKNOWLEDGEMENTS

We like to thank **Judith Petri** for the previous work and reactions on the behavior of the acrylates. Further, we like to thank **Andreas Böttcher** from the mechanical workshop for designing the QCM cell and the lid for the reactor.

NOMENCLATURE

d	Thickness, m
f	Frequency, Hz
m	Mass, kg
\dot{m}	Rate of mass change, kg/(m ² ·s)
n	Overtone order
R_f	Fouling resistance, m ² ·K/W
t	Time, s
Γ	Half bandwidth at half height, Hz
κ	Spring constant, kg/s ²
λ_d	Thermal conductivity, W/m·K
λ	Wavelength of shear sound, m
ρ	Density, kg/m ³

Subscript

eff	effective
d	Deposit
f	Film
l	Layer
q	Quartz
r	Removal
ref	Reference

REFERENCES

- [1] Hungenberg, K.-D. and Jahns, E., Trends in Emulsion Polymerization Processes from an Industrial Perspective, in *Polymer Reaction Engineering of Dispersed Systems*, W. Pauer, Ed., Cham: Springer International Publishing, pp. 195–214, 2017.
- [2] Lovell, P. A. and Schork, F. J., Fundamentals of Emulsion Polymerization, *Biomacromolecules*, vol. **21**, no. 11, pp. 4396–4441, 2020.
- [3] Erbil, H. Y., Vinyl Acetate Emulsion Polymerization and Copolymerization with Acrylic Monomers, CRC Press, pp. 336, 2000.
- [4] Asua, J. M., Emulsion Polymerization: From Fundamental Mechanisms to Process Developments, *Journal of Polymer Science Part A: Polymer Chemistry*, vol. **42**, no. 5, pp. 1025–41, 2004.
- [5] Pauer, W., Reactor Concepts for Continuous Emulsion Polymerization, in *Polymer Reaction Engineering of Dispersed Systems: Volume I*, W. Pauer, Ed., Cham: Springer International Publishing, pp. 1–17, 2018.
- [6] Urrutia, J. and Asua, J. M., Reactor Fouling in Emulsion Polymerization, *Industrial & Engineering Chemistry Research*, vol. **60**, no. 29, pp. 10502–10, 2021.
- [7] Watkinson, A. P. and Wilson, D. I., Chemical Reaction Fouling: A Review, *Experimental Thermal and Fluid Science*, vol. **14**, no. 4, pp. 361–74, 1997.
- [8] Urrutia Fernández de Retana, J., Fouling in Emulsion Polymerization Reactors, Ph.D. thesis, University of the Basque Country UPV/EHU, Spain, 2016.
- [9] Epstein, N., Thinking about Heat Transfer Fouling: A 5×5 Matrix, *Heat Transfer Engineering*, vol. **4**, no. 1, pp. 43–56, 1983.
- [10] Müller-Steinhagen, H., Heat Transfer Fouling: 50 Years After the Kern and Seaton Model, *Heat Transfer Engineering*, vol. **32**, no. 1, pp. 1–13, 2011.
- [11] Wallhäußer, E., Hussein, M. A. and Becker, T., Detection Methods of Fouling in Heat Exchangers in the Food Industry, *Food Control*, vol. **27**, no. 1, pp. 1–10, 2012.
- [12] Böttcher, A., Petri, J., Langhoff, A., Scholl, S., Augustin, W., Hohlen, A. and Johannsmann, D., Fouling Pathways in Emulsion Polymerization Differentiated with a Quartz Crystal Microbalance (QCM) Integrated into the Reactor Wall, *Macromolecular Reaction Engineering*, vol. **16**, no. 2, p. 2100045, 2022.
- [13] Sauerbrey, G., Verwendung von Schwingquarzen zur Wägung dünner Schichten und zur Mikrowägung, *Zeitschrift für Physik*, vol. **155**, no. 2, pp. 206–22, 1959.
- [14] Johannsmann, D., Langhoff, A. and Leppin, C., Studying Soft Interfaces with Shear Waves: Principles and Applications of the Quartz Crystal Microbalance (QCM), *Sensors*, vol. **21**, no. 10, p. 3490, 2021.
- [15] Niaounakis, M., *Biopolymers: Processing and Products*, M. Niaounakis, Ed., Oxford: William Andrew Publishing, pp. 85–117, 2015.
- [16] Johannsmann, D., Petri, J., Leppin, C., Langhoff, A. and Ibrahim, H., Particle Fouling at Hot Reactor Walls Monitored In Situ with a QCM-D and Modeled with the Frequency-Domain Lattice Boltzmann Method, *Results in Physics*, vol. **45**, p. 106219, 2023.
- [17] Kugimoto, D., Kouda, S. and Yamaguchi, M., Modification of Poly(Lactic Acid) Rheological Properties Using Ethylene-Vinyl Acetate Copolymer, *Journal of Polymers and the Environment*, vol. **29**, no. 1, pp. 121–29, 2021.
- [18] Münstedt, H., Various Features of Melt Strain Hardening of Polymeric Materials in Uniaxial Extension and Their Relation to Molecular Structure: Review of Experimental Results and Their Interpretation, *Rheologica Acta*, vol. **62**, no. 7, pp. 333–63, 2023.